

Madagascar satellite data: an inversion test case

Jesse Lomask¹

ABSTRACT

The Madagascar satellite data set provides images of a spreading ridge off the coast of Madagascar. This data set has two regions: the southern half is densely sampled and the northern half is sparsely sampled. This data set is an excellent test case for inversion methods. It presents several challenges that geophysicists face in generating seismic maps in general. The data is acquired in swaths that follow irregular paths(tracks), similar in some respects to irregular 3D acquisition geometries. Inversion allows us to combine these different data paths into one image. Shifts between tracks are removed by taking the derivative along the tracks in the inversion fitting goals. By looking at the residual in data-space, we were able to see errors in the weighting operator. The sparsely sampled region presents a missing data problem. In the future, we intend to estimate 2D prediction error filters (PEFs) on these sparse tracks and use them to fill in the missing data. I have tested one method on a simple 1D model, in which I estimate a PEF and missing data simultaneously while throwing out fitting equations where the leading 1 coefficient of the PEF lands on unknown data. Thus, this data will give us an opportunity to test different methods of estimating PEFs on sparse and irregular data. Also, preconditioning on the helix greatly speeds convergence.

INTRODUCTION

To a certain extent, the surface of the ocean is a gravitational equipotential surface. Mountains and ridges beneath cause bulges in the sea surface which reflect the topography beneath. With each pass, the GEOSAT satellite measures thin swaths of the height of the sea-level above some reference ellipsoid. Numerous passes can be combined to create a map of the ocean floor topography (Lomask, 1998). The altimetry of the sea surface is also influenced by tidal fluctuations and currents that overwhelm the high frequency bulges that we are interested in imaging. Any two adjacent or crossing tracks are mismatched by a low or zero frequency shift.

The satellite data consists of four different sets, each of which is a one-dimensional array of tracks connected end to end. There are two sets of sparsely sampled tracks, one north flying and one south flying. There are also two sets of densely sampled tracks, again one north flying (ascending) and the other south flying (descending). The sparse tracks cover the same region as the dense tracks plus a region of equal size to the north. Figure 1 shows the geometry of the data separated into sparse tracks and dense tracks.

¹email: lomask@sep.Stanford.EDU

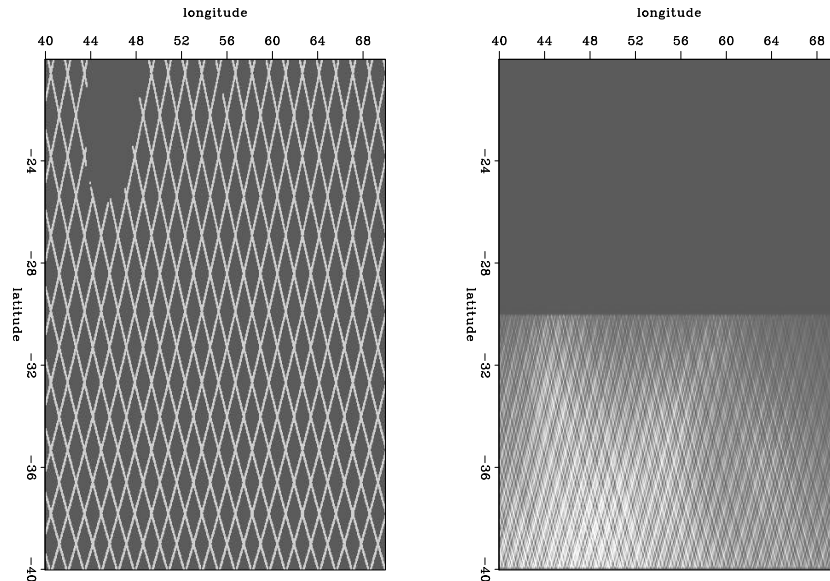


Figure 1: The raw binned data. Left is the raw normalized sparse tracks. The gap at the top is the island of Madagascar. Right is the raw dense tracks. `jesse2-tracks` [ER]

Using a weighted least squares approach, Ecker and Berlioux (1995) imaged the dense southern region. They used a derivative along the data tracks to remove the shifts between each pass. Some work has been done to image the sparse tracks. Lomask (1998) estimated 2D prediction error filters (PEFs) on the dense region and applied them in regularization operators on the sparse region. In this paper, I review how inversion is used to image the Madagascar data. Also, I describe methods for estimating and applying PEFs on sparse and irregular data.

A good test case for inversion

The Madagascar satellite data is an excellent test case for seismic inversion methods because it poses several challenges that occur regularly in making seismic maps. This data was recorded on thin, curved swaths creating complications similar to the irregular geometry commonly seen in 3D seismic acquisition. This could be cable feathering on marine data or irregular land geometries cause by obstructions. As will be shown in more detail later, the fact that there are both ascending and descending tracks presents a problem of combining two different types of data to image one geological event. Furthermore, this data has two data densities, the northern sparsely sampled region and the southern densely sampled region. Balancing the weighting of these two data densities adds complexity to the inversion fitting goals. Additionally, the sparsely sampled region poses a challenging missing data problem especially because the sparse tracks are not oriented parallel to any axis. Lastly, the Madagascar data makes a good test case because of the clarity of the image itself. If the data is processed incorrectly, it is usually obvious that a mistake was made. However, as we will see later, this is not always the case.

BACKGROUND

In petroleum geophysics, one geological event can be imaged with multiple data types. For instance, the top of a reservoir can be mapped with multiple seismic surveys and multiple well log runs. Inversion can be used to create a single model of the top of the reservoir to satisfy these diverse data. The Madagascar data set can be viewed as a similar problem. Figure 2 illustrates this point on only the densely sampled data. The Madagascar data can be imaged by taking the derivative along the tracks and binned. The derivative along both the ascending tracks and the descending tracks individually provides an image of the ridge. Combining both data sets to create one model of the ridge can be achieved with inversion.

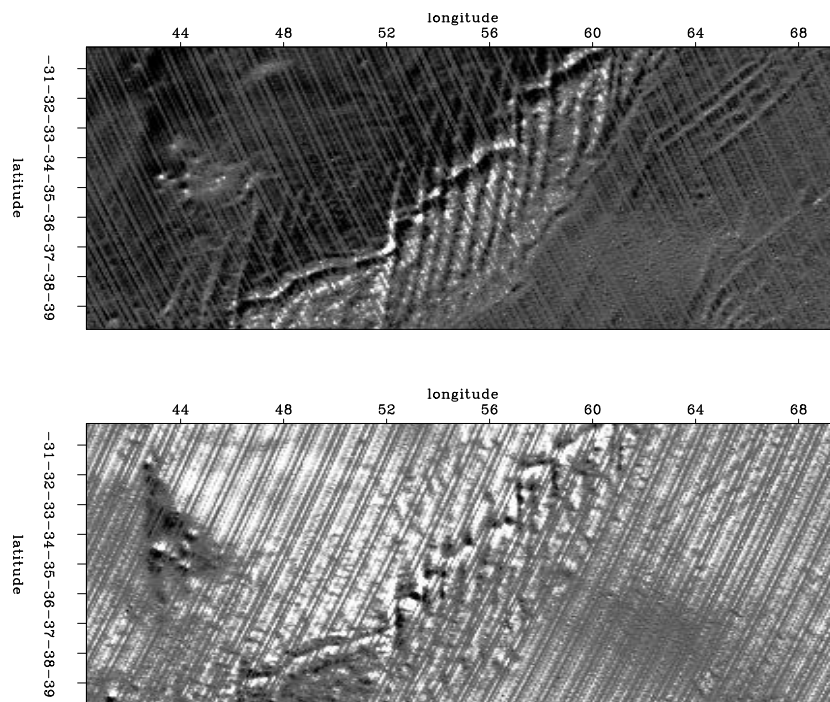


Figure 2: Dense data: ascending (top) and descending (bottom) tracks with gradient `jesse2-updwnder1` [ER,M]

Fitting goals

As described in Lomask (1998), we use inversion to find the model (\mathbf{m}) that when sampled into data-space using linear interpolation (\mathbf{L}) will have a derivative ($\frac{d}{dt}$) that will equal the derivative of the data (\mathbf{d}). \mathbf{W} is a weighting operator that merely throws out fitting equations that are contaminated with noise or track ends. Expressed as a fitting goal, this is :

$$\mathbf{W} \frac{d}{dt} [\mathbf{Lm} - \mathbf{d}] \approx \mathbf{0}. \quad (1)$$

For the sparse tracks or missing bins, we add a regularization fitting goal to properly fill in the data. Our fitting goals are now:

$$\begin{aligned} \mathbf{W} \frac{d}{dt} [\mathbf{Lm} - \mathbf{d}] &\approx \mathbf{0} \\ \epsilon \mathbf{Am} &\approx \mathbf{0}. \end{aligned} \quad (2)$$

Applying these goals on the dense data, we get the smooth result in Figure 3.

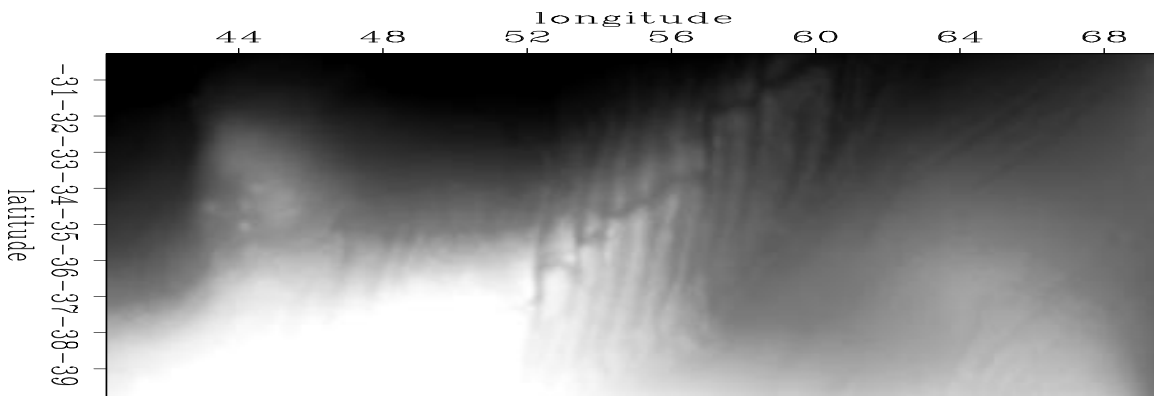


Figure 3: Result of applying fitting goals (equation 2). `jesse2-fulldenseNoRuf` [ER]

To make it look more interesting, we roughen the model by taking the first derivative in the east-west direction as in Figure 4. This highlights a lot of the minor north-south oriented ridges. Similarly, we can roughen it in the north-south direction as in Figure 5. This highlights the central main ridge. Applying the helical derivative, we get the results in Figure 6. Unlike the directional derivative operators, this highlights features with less directional bias. Lastly, we take the east-west second derivative to get the very crisp image in Figure 7.

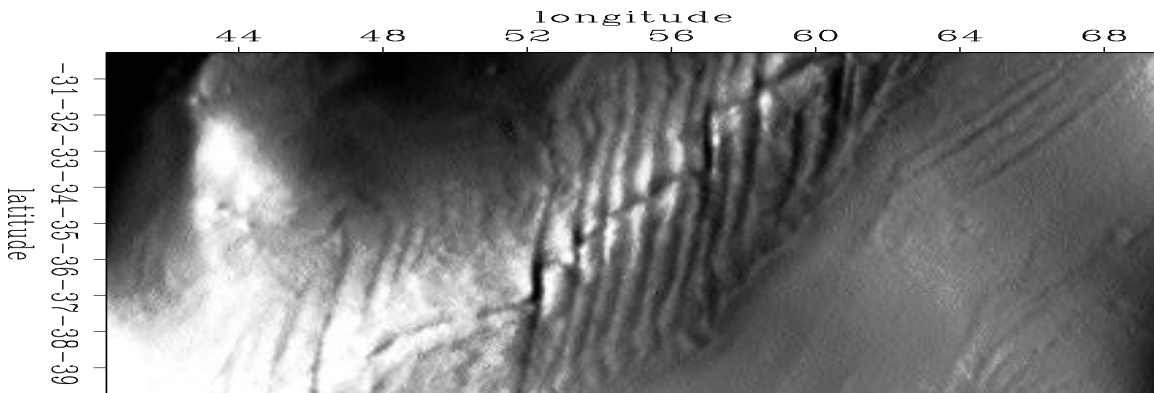


Figure 4: Results of fitting goals with east-west derivative. `jesse2-fulldense1` [ER]

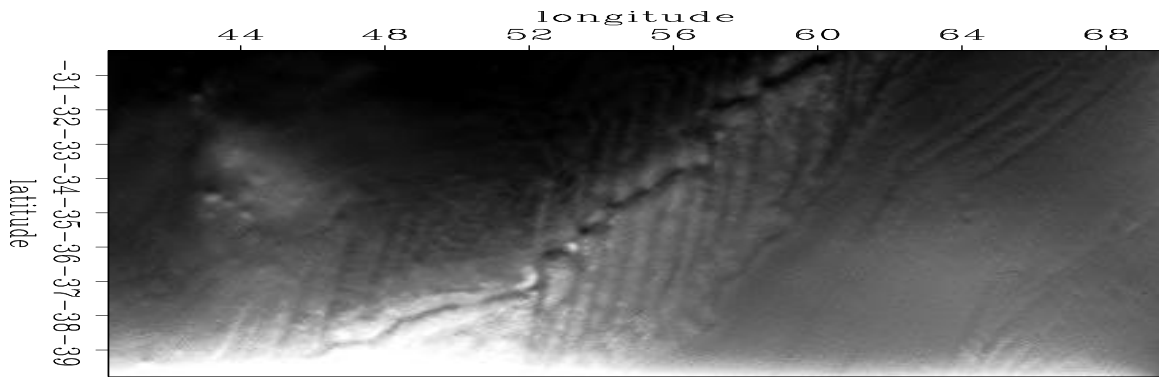


Figure 5: Results of fitting goals with north-south derivative. `jesse2-fulldenseNS1` [ER]

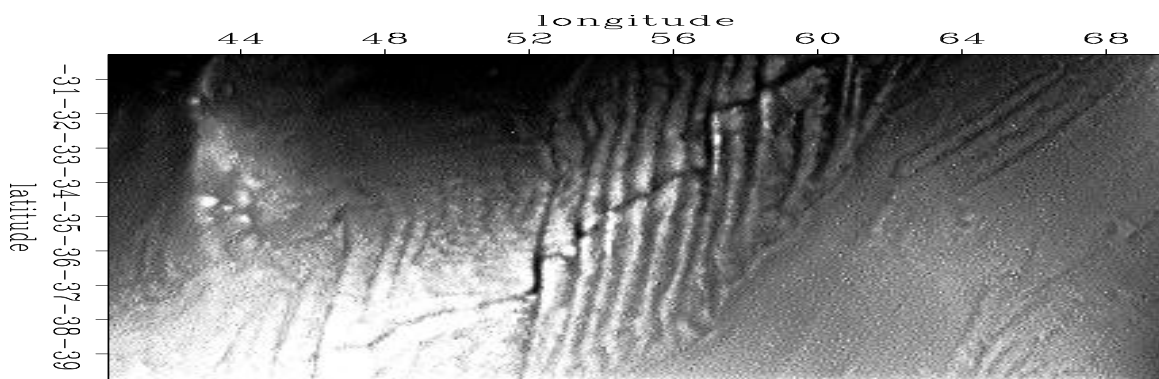


Figure 6: Results of fitting goals with helix derivative. `jesse2-helix` [ER]

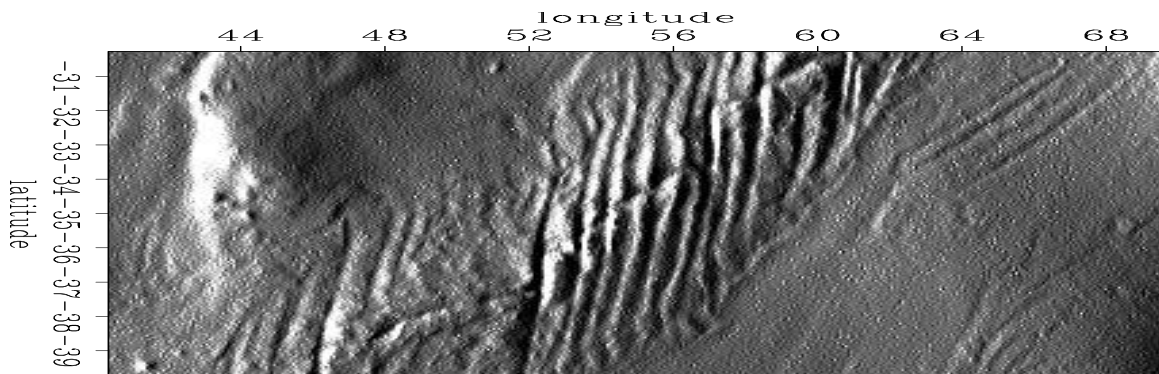


Figure 7: Results of fitting goals with east-west 2nd derivative. `jesse2-fulldense2nd1` [ER]

LOOKING AT DATA-SPACE

Even in the case of the Madagascar data set, just looking at the output model is not enough to determine the quality of the result. In this case, there were inaccuracies in the weight, \mathbf{W} , that were allowing some bad data points to slip into the fitting equations. There were only a few, so the model still looked good but observation of the data-space residual alerted us to a problem. Figure 9 shows the residual after convergence. The differences between each track should be constant, or near constant, shifts, so you would expect the residual to be comprised of constant or near constant shifts. This residual has a lot of curved features which were the result of the solver trying to fit the model to some bad data and spreading the errors out over the model.

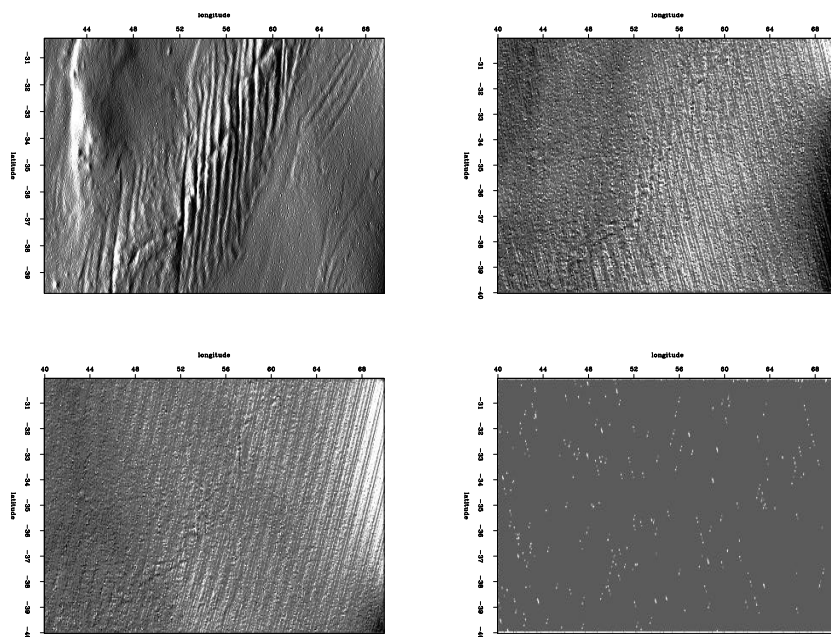


Figure 8: Top left: model roughened with east-west 2nd derivative. Top right: residual of ascending tracks with gradient applied then binned into model-space. Bottom left: residual of descending tracks with gradient applied then binned into model-space. Bottom right: binned weight. `jesse2-badmovie` [ER,M]

To see if there was a model space correlation in the position of the residual curves, I separated the residual into ascending and descending tracks, took the derivative along the tracks, and binned them. I took the derivative along the tracks to highlight steep or curved features. Figure 8 shows the binned residual. Notice the brightening and dimming on the right side of the ascending and descending tracks, respectively. This means that the curved features are all lining up on the right (west) side of the map. Then I looked at the binned weight and right away saw that there were no 0's on the right side of the map. Upon further examination it became clear that I was clipping the weight in model space, thus allowing all of the track ends along the right side of the map to slip into our fitting equations.

After correcting the problem, the residual looks more like it should as in Figure 11. Also

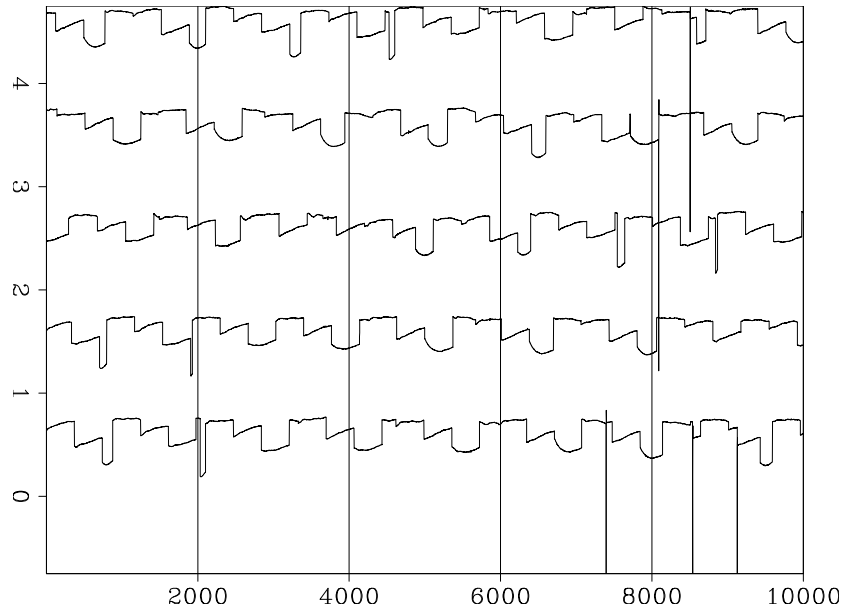


Figure 9: Residual from a group of tracks using incorrect weight. Curved features look very suspicious. `jesse2-resmovie_bad` [ER,M]

the binned residual looks whiter and without the brightening and dimming as in Figure 10. Figure 12 compares the model with the correct weight to the model with the incorrect weight. The difference is slight, basically just a flexing on the right side of the map.

ESTIMATING PEF ON RESIDUAL

We used the first derivative in our fitting goal to remove the shifts between tracks. As was done previously in Lomask (1998), I tested the nature of the residual by estimating a 1D PEF on it, to see if correcting the weighting operator made difference. If the estimated PEFs are not first derivatives, then we would want to use one of them in our fitting goals instead of $\frac{d}{dt}$. The PEFs look like first derivatives, but in the case of the PEFs with more than three terms, it isn't obviously a first derivative. We will need to look at the impulse response of the inverse PEF to get a better idea of the nature of the PEFs.

PEF	Coef 1	Coef 2	Coef 3	Coef 4	Coef 5
2 terms	1.00	-1.00	-	-	-
3 terms	1.00	-1.06	0.055	-	-
4 terms	1.00	-1.08	0.497	-0.419	-
5 terms	1.00	-1.08	0.284	-0.258	0.050
10 terms	1.00	-1.07	0.270	-0.227	0.028
	-0.019	-0.014	0.001	-0.035	0.053

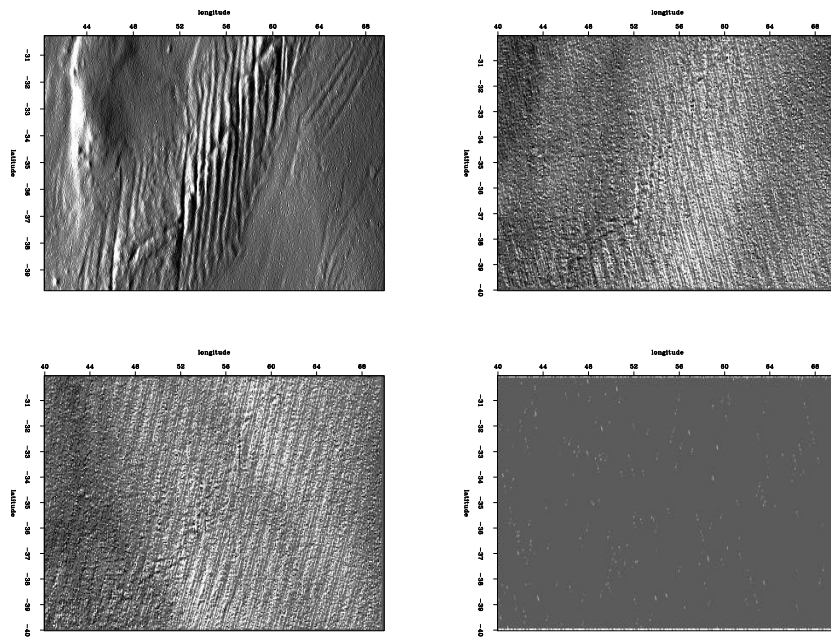


Figure 10: Top left: corrected model roughened with east-west 2nd derivative. Top right: residual of ascending tracks with gradient applied then binned into model-space. Bottom left: residual of descending tracks with gradient applied then binned into model-space. Bottom right: binned corrected weight. `jesse2-goodmovie` [ER,M]

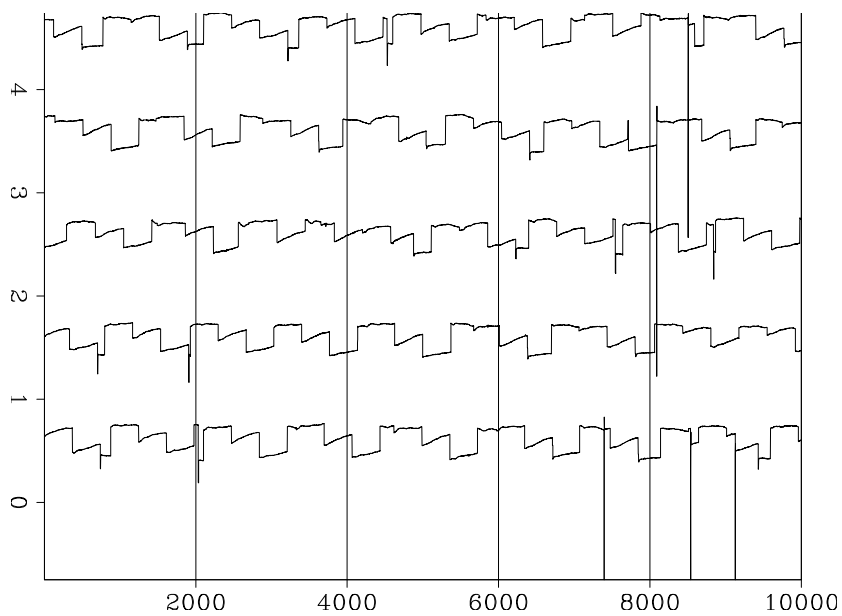


Figure 11: Residual from a group of tracks using corrected weight. `jesse2-resmovie_good` [ER,M]

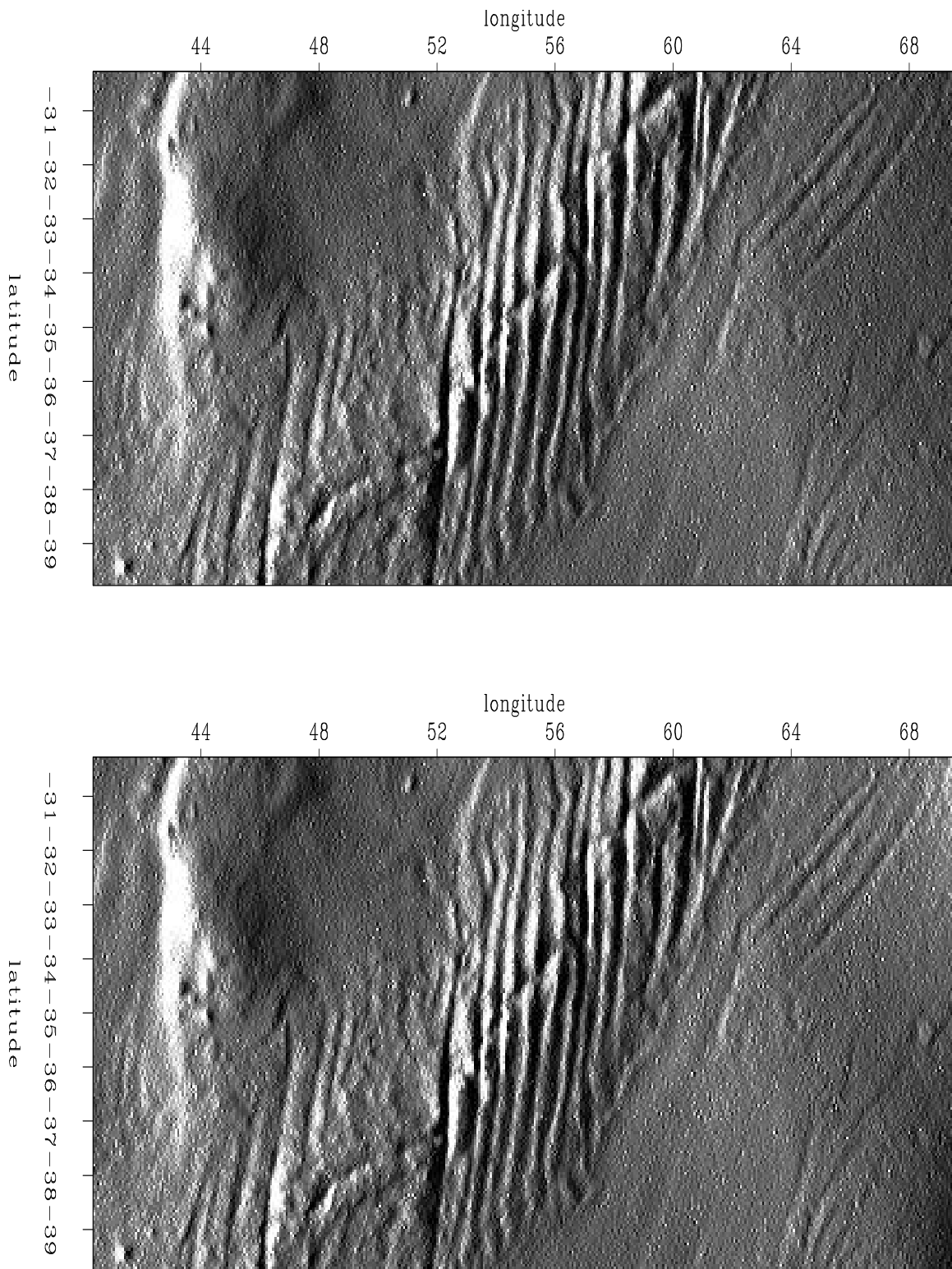


Figure 12: Top: model with corrected weight roughened with east-west 2nd derivative. Bottom: model with original weight roughened with east-west 2nd derivative.

`jesse2-goodandbad` [ER,M]

DEALING WITH SPARSE DATA

The sparse tracks present a problem that is seen a lot in geophysics. We have a non-stationary geological surface, in this case the surface of the ocean. We have missing data, in this case the gaps between the tracks. Our known data is along irregular geometries, the sparse tracks themselves. Previous results in the sparse region were regularized with PEFs estimated on the dense region (Lomask, 1998). Now, we would like to deal only with the sparse data. Our goal is to estimate a filter on the the known sparse data and use it to fill the missing data. Ideally, we could estimate two 1D filters; one on the ascending sparse tracks and one on the descending sparse tracks. In the real world, this would be problematic because the geometry of the tracks is irregular.

Possible solutions

One possible solution would be to estimate a 2D PEF using multi-scale PEF estimation (Curry and Brown, 2001). Another possibility would be to estimate both a 2D PEF and the missing data at the same time in a similar approach to equation 3 from Claerbout (1999) but instead of estimating the PEF everywhere, throw out all fitting equations where the leading 1 of the PEF lands on unknown data. If you were to throw out all fitting equations where any coefficient of the PEF lands on unknown data, there would not be enough fitting equations to actually calculate the PEF. To estimate the PEF (\mathbf{a}) on a model (\mathbf{y}), we start with an initial model convolved with an initial filter ($\mathbf{A}\mathbf{y}$) and perturb them with $\Delta\mathbf{y}$ and $\Delta\mathbf{a}$. In equation 4 we add the residual weight, \mathbf{W} , to throw out fitting equations where the first coefficient of \mathbf{a} lands on missing data. The free-mask matrix for missing data is denoted \mathbf{J} and that for the PEF is \mathbf{K} .

$$\mathbf{0} \approx \begin{bmatrix} \mathbf{A} & \mathbf{J} & \mathbf{Y} & \mathbf{K} \end{bmatrix} \begin{bmatrix} \Delta\mathbf{y} \\ \Delta\mathbf{a} \end{bmatrix} + \mathbf{A}\mathbf{y} \quad (3)$$

$$\mathbf{0} \approx \mathbf{W} \begin{bmatrix} \mathbf{A} & \mathbf{J} & \mathbf{Y} & \mathbf{K} \end{bmatrix} \begin{bmatrix} \Delta\mathbf{y} \\ \Delta\mathbf{a} \end{bmatrix} + \mathbf{A}\mathbf{y} \quad (4)$$

In Claerbout (1999), Figure 13 is generated by estimating both the missing data and unknown filter at the same time. I added a data-space weight as above and got the results in Figure 14. Notice it almost calculates the same filter. It does not completely fill in the missing data because we threw out many fitting equations.

I have tested this only on simple 1D models, not yet on the Madagascar data. For the Madagascar data, the initial filter (\mathbf{a}) may be the Laplacian.

Figure 13: Top is known data. Middle includes the interpolated values. Bottom is the filter with the left-most point constrained to be unity and other points chosen to minimize output power. `jesse2-misif90` [ER]

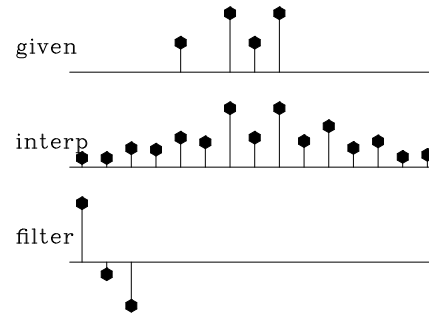
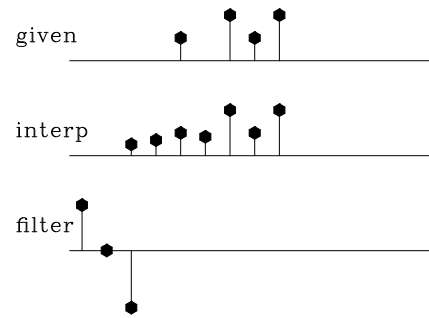


Figure 14: Top is known data. Middle includes the interpolated values. Bottom is the filter with the left-most point constrained to be unity and other points chosen to minimize output power but only throwing out fitting equations where the left-most point lands on unknown data. `jesse2-misif90_2` [ER]



PRECONDITIONING

Here I applied preconditioning on the helix using the following fitting goals (Fomel, 1997):

$$\text{substitute } \mathbf{m} = \mathbf{A}^{-1}\mathbf{p} \quad (5)$$

$$\mathbf{W} \frac{d}{dt} [\mathbf{L}\mathbf{A}^{-1}\mathbf{p} - \mathbf{d}] \approx \mathbf{0} \quad (6)$$

$$\epsilon \mathbf{p} \approx \mathbf{0}$$

In this case, a 2D PEF was estimated on the dense tracks and applied as regularization to the sparse tracks. This greatly improved the speed of convergence to create Figure 15.

SUMMARY

As a small, non-stationary data set with irregular acquisition geometry, the Madagascar satellite data has allowed us to gain some valuable insight into inversion pitfalls and challenges. By looking at the data-space residual, an error was discovered. The impact of this error on the bootstrapping process of choosing the appropriate filter (in this case, $\frac{d}{dt}$) to remove the shift between tracks was minimal.

The use of this data is still not fully exploited. By understanding how to estimate filters on the sparse tracks and use them to fill in the sparse area, we will better understand how to tackle similar problems that arise regularly in seismic map generation.

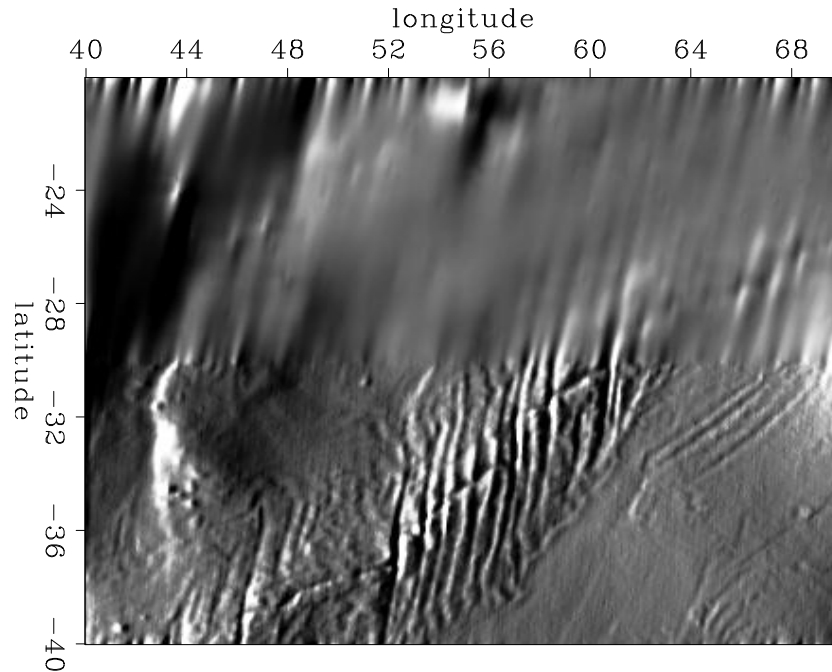


Figure 15: Result of fitting goal 6 applied to both sparse and dense data together using a 2D PEF estimated on dense data. [jesse2-madfig7](#) [ER]

ACKNOWLEDGMENTS

I would like to thank Jon Claerbout for ideas and suggestions. I would also like to thank Bill Curry and Bob Clapp for help de-bugging code and useful discussions.

REFERENCES

- Claerbout, J., 1999, Geophysical estimation by example: Environmental soundings image enhancement: Stanford Exploration Project, <http://sepwww.stanford.edu/sep/prof/>.
- Curry, W., and Brown, M., 2001, A new multiscale prediction-error filter for sparse data interpolation: SEP-110, 113–122.
- Ecker, C., and Berlioux, A., 1995, Flying over the ocean southeast of Madagascar: SEP-84, 295–306.
- Fomel, S., 1997, On model-space and data-space regularization: A tutorial: SEP-94, 141–164.
- Lomask, J., 1998, Madagascar revisited: A missing data problem: SEP-97, 207–216.